

Si-Based Photonic Crystals and Photonic-Bandgap Waveguides

Masaya NOTOMI^{†a)}, Akihiko SHINYA[†], Eiichi KURAMOCHI[†], *Nonmembers*,
 Itaru YOKOHAMA[†], *Regular Member*, Chiharu TAKAHASHI^{††}, Koji YAMADA^{†††},
 Jun-ichi TAKAHASHI^{†††}, Takayuki KAWASHIMA^{†††}, *Nonmembers*,
 and Shojiro KAWAKAMI^{†††}, *Regular Member*

SUMMARY We studied various types of 2D and 3D Si-based photonic crystal structures that are promising for future photonic integrated circuit application. With regard to 2D SOI photonic crystal slabs, we confirmed the formation of a wide photonic bandgap at optical communication wavelengths, and used structural tuning to realize efficient single-mode line-defect waveguides operating within the bandgap. As regards 3D photonic crystals, we used a combination of lithography and the autocloning deposition method to realize complicated 3D structures. We used this strategy to fabricate 3D full-gap photonic crystals and 3D/2D hybrid photonic crystals.

key words: photonic crystal, photonic band gap, waveguide, photonic IC, Si photonics

1. Introduction

Photonic crystals have various unique optical properties [1], [2] and are thus considered promising candidates as key platforms for future ultra-small large-scale photonic integrated circuits (PICs). It has been theoretically predicted that various optical properties of photonic crystals are advantageous as regards this goal.

The selection of component materials is very important if we are to realize PICs by using photonic crystals. With conventional optoelectronic circuits (such as III-V semiconductor PICs or silica planar lightwave circuits [3]), a relatively small refractive index difference is normally used to reduce the scattering loss, and fine index variation is essential to PIC design. This means that Si is not a good choice for optoelectronic use because fine index modulation is difficult.

The situation is different with photonic-crystal-based PICs, where a large index difference is essential if we are to realize field confinement using photonic bandgap (PBG) effects. In this case, we design the circuits (e.g., waveguides, resonators) not by tuning the

index variation, but by tuning the defect structures in photonic crystals. In such a situation, Si is an ideal material despite the conventional belief that it is unsuitable for optoelectronic use. Si offers several advantages. We can employ state-of-the-art nano-fabrication technologies for Si, there are various technologies for realizing a combination of Si and SiO₂, which is ideal for obtaining a large index difference, and Si is compatible with VLSI chips.

For these reasons, Si is a promising material with a view to developing photonic crystal-based PICs. Next, we consider the photonic crystal structure. There are two possible ways to realize photonic-crystal-based PICs, namely through the use of 2D or 3D photonic crystals (1D photonic crystals are almost useless for this purpose). It might seem that simple 2D photonic crystals are sufficient for constructing PICs because normal circuits are 2D. However, we have to introduce a certain degree of strong confinement in the third (vertical) dimension in order to confine the light field effectively inside the photonic crystals, and thus we have to design 3D structures.

One of simplest structures satisfying this requirement is the 2D photonic crystal slab structure shown in Figs. 1(a), (b), which can be fabricated by current lithographic techniques and is currently the most extensively studied. This photonic crystal slab is a thin, high refractive-index semiconductor slab, which is periodically structured and sandwiched between cladding layers (typically air [4] or oxide [5]) with a low refractive index. Vertical confinement is realized by adopting a large index contrast between the slab and cladding.

Photonic crystal slabs already have most of the functions expected of photonic crystal-based PICs, and they are much easier to fabricate than 3D PICs. Therefore, we believe that 2D photonic crystal slabs are currently the most promising structures with which to construct photonic crystal ICs. It is also true, however, that 3D photonic crystals will ultimately be the ideal. 3D photonic crystals are greatly superior to 2D crystals especially when we require a very large Q-factor for point defects or we are concerned with the control of the light emission process.

With the above as the background, we are studying several types of Si-based photonic crystal structure.

Manuscript received October 3, 2001.

Manuscript revised November 21, 2001.

[†]The authors are with NTT Basic Research Labs., NTT Corporation, Atsugi-shi, 243-0198 Japan.

^{††}The author is with NTT Advanced Technology/NTT Telecommunication Energy Labs., NTT Corporation, Atsugi-shi, 243-0198 Japan.

^{†††}The authors are with NTT Telecommunications Energy Labs., NTT Corporation, Atsugi-shi, 243-0198 Japan.

^{††††}The authors are with NICHe, Tohoku University, Sendai-shi, 980-8579 Japan.

a) E-mail: notomi@will.brl.ntt.co.jp

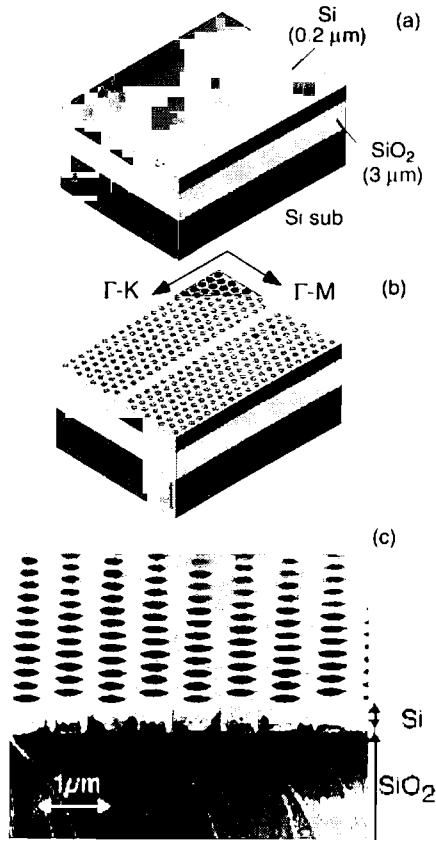


Fig. 1 Schematics and SEM micrograph of 2D photonic crystal slabs. (a) bulk. (b) line defect. (c) SEM micrograph.

First one is a 2D silicon-on-insulator (SOI) photonic crystal slab that we fabricated from high-quality SOI substrates by using state-of-the-art Si nano-fabrication technology. In addition, we are also studying 3D Si/SiO₂ photonic crystals that are predicted to exhibit a full PBG at optical communication wavelengths and that can be fabricated by a fairly simple process. Furthermore, we combine these two technologies and fabricate 3D/2D hybrid photonic crystals.

2. SOI Photonic Crystal Slab

Figure 1(c) shows an SEM micrograph of fabricated 2D SOI photonic crystals. A hexagonal air-hole pattern was formed in a high-quality SOI substrate by e-beam lithography and ECR ion-stream etching [6], [7]. With regard to 2D photonic crystals, the most important issue is determining the best way to confine the light in the vertical direction. The Si layer thickness (0.2 μm) is designed to satisfy the single-mode condition in the vertical direction.

Our structure is an SOI-type photonic crystal slab with a SiO₂ cladding layer underneath [8]. Although air-bridge-type photonic crystal slabs with air cladding for both the upper and lower layers have been widely studied [9], our SOI photonic crystal is more suitable for

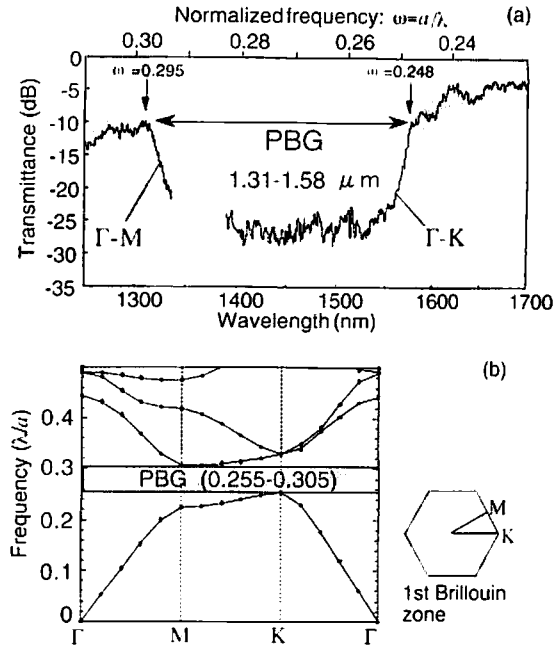


Fig. 2 (a) Transmission spectrum of the bulk SOI photonic crystal slab with two crystal-axis orientations (Γ -K and Γ -M). (b) Calculated photonic band diagram of the same SOI photonic crystal slab. The lattice constant $a = 0.39 \mu\text{m}$ and the hole diameter is $0.55a$. A reciprocal space representation of the lattice is also shown.

device applications and easy to extend over a large-scale area. But it has been theoretically pointed out that asymmetric photonic crystal slabs such as the SOI-type are inefficient as regards possessing a PBG for either polarization because the asymmetry leads to polarization mixing and this breaks up the PBG. We estimated this coupling effect for SOI photonic crystal slabs with hexagonal air holes by using the 3D finite-difference time-domain (FDTD) method, and found that the lowest PBG for TE-like modes rejects the TE incident wave with an extinction ratio of more than 35 dB [10].

If we wish to construct photonic crystal-PICs, we must first confirm whether appropriate PBGs are formed at desired wavelengths. This is not an easy experiment because we have to couple light to a very thin slab and measure the transmittance over a wide frequency range. Thus, there have been very few experimental results related to this important information. We have directly measured the transmittance of 2D SOI photonic crystals by using a single-mode tapered fiber and a wide-band white light source. Figure 2 shows transmittance spectra along two crystal axes and the corresponding photonic band diagram for TE polarization. We observed a common PBG from 1.31 to 1.58 μm for Γ -K and Γ -M orientations, which shows that a full PBG is open in the 2D plane. The experimental result agrees very well with the 3D FDTD calculation [11].

The observed PBG covers the entire wavelength range currently used for optical communications. Thus,

this result shows that SOI photonic crystal slabs can be considered as possible platforms for PICs in this wavelength range.

3. Photonic-Bandgap Waveguides

3.1 Design

The previous result showed that SOI photonic crystal slabs have an effective PBG. We next introduce functional defects operating within the PBG. In photonic crystals with PBGs, a line defect can operate as a tightly confined waveguide and a point defect can be an ultra-small high-Q cavity [12]. In this study, we examine line defect waveguides operating within PBGs. Although there have been several studies on line defect waveguides [13]–[15], few have provided quantitative measurements and discussion.

The operating principles of line defect waveguides within PBG frequencies (PBG waveguides) are very different from those of conventional dielectric waveguides. PBG waveguides have a large degree of freedom with regard to tuning such waveguiding characteristics as mode dispersion. Therefore, PBG waveguide design is very important.

When designing the waveguiding modes of line defects in photonic crystal slabs, we have to consider two issues: group velocity and light line. To realize efficient PBG waveguides, it is desirable to have a single waveguiding mode with sufficient group velocity under the light line of the cladding within the PBG region. This is hard to achieve for the normal single-missing-hole line defect of an SOI photonic crystal slab. Therefore, we have already proposed various ways of tuning the geometrical structure of line defects so that the guiding mode realizes the above characteristics.

In this study, we chose the simplest tuning method, namely control of the line defect width. We studied the effect of tuning the defect width with 2D calculations. For experimental studies, we have to perform 3D calculations to design the structural parameters of the samples. So here we used the 3D FDTD method to calculate the waveguiding characteristics of the line defects. Note that 3D FDTD calculations yield information not only about true waveguiding modes but also about quasi-waveguiding modes (i.e., leaky modes) above the light line [16]. For example, we can calculate the lifetime (propagation loss) of leaky modes. We used a periodic boundary condition in the propagation direction and a perfectly matched layer boundary condition for other directions.

Figure 3 shows calculated dispersion curves of normal single-missing-hole line defects and width-reduced line defects. Here, we define the width of defect w_d as the spacing between the centers of holes nearest the defect, and the width of normal line defect w_d as W ($=\sqrt{3}a$). The width w_d in Fig. 3(b) is $0.7W$. Nor-

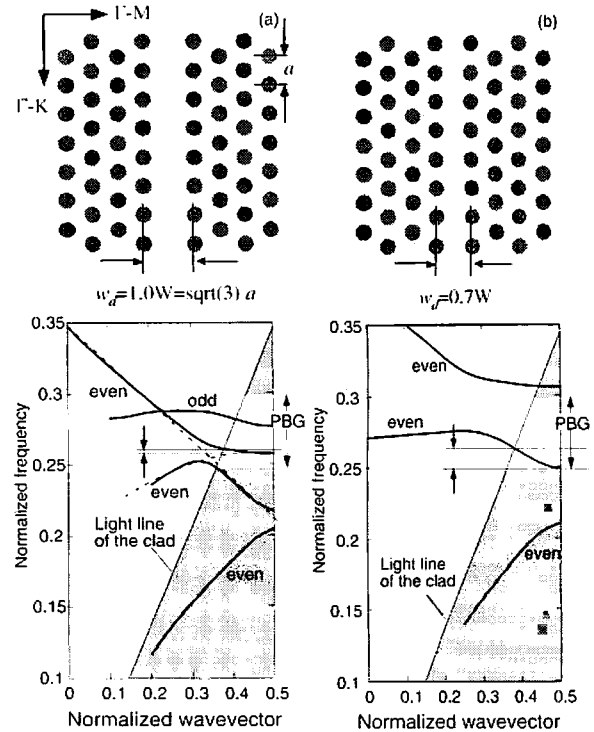


Fig. 3 Calculated dispersion curves of line defects in photonic crystal slabs calculated by the 3D FDTD method: (a) normal single-line defect ($w_d = 1.0W$) in SOI hexagonal air-hole photonic crystal slab. Broken lines show hypothetical index-guided and gap-guided modes that are the origin of the mode within the PBG. (b) width-reduced single-line defect ($w_d = 0.7W$) in SOI hexagonal air-hole photonic crystal slab. The pale shaded area corresponds to the region inside the light cone of the cladding, where modes become leaky, and the dark shaded area corresponds to the region outside the PBG.

mal line defects have at least two modes (even and odd) in the PBG. It is clearly seen that an even waveguiding mode with the PBG for normal line defects has a very small group velocity under the light line of the cladding (the area indicated by two vertical arrows). This small group velocity leads to a small transmission window and also means that this mode might prove very susceptible to structural disorder, which must be present in the real samples. We attribute the origin of this small group velocity to the fact that strong anticrossing occurs between the index-guided mode and the gap-guided mode around this region (they are shown by broken lines in the plot, and are the origin of the waveguiding mode in the PBG). Therefore, the position and strength of this anticrossing can be significantly changed by employing properly designed structural tuning [17].

By contrast, width-reduced line defects ($w_d = 0.7W$) in the same photonic crystal slab have a single waveguiding mode with a sufficiently large group velocity under the light line within the PBG. This leads to a larger transmission window (the transmission win-

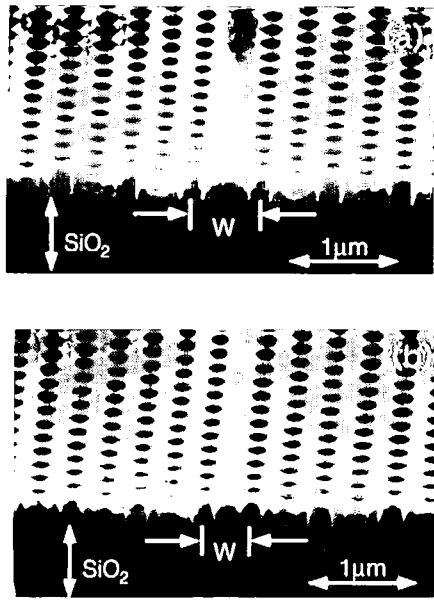


Fig. 4 SEM micrographs of width-controlled line defects of 2D SOI photonic crystal slabs. (a) normal width ($w = 1.0W$). (b) reduced width ($w = 0.70W$).

dow is indicated by two vertical arrows determined from the lower mode edge and the intersecting point of the mode curve and the light line). The improvement seen in this 3D calculation is basically consistent with the 2D calculation. By using this 3D calculation result, we determined the structural parameters of the width-reduced line defects (The fabricated structure is shown in Fig. 2). In addition, this 3D calculation directly shows that the waveguiding mode of width-reduced waveguides is truly single-mode even if we take leaky modes above the light line into account. This feature is very important for practical applications.

We fabricated a variety of width-controlled line defects in SOI photonic crystal slabs [18], as shown in Fig. 4. The fabrication process is basically the same as that described in Sect. 2.

3.2 Transmission Spectra of Line Defects

(a) Normal line defects

We measured the transmission spectra of line defects with the same tapered fiber set-up that we used for bulk photonic crystal samples. The input light was directly coupled to the cleaved edge of the line defects, and the output signal was collected from the output port of 10- μm -wide stripe waveguides. The measured transmission spectrum is shown in Fig. 5(a), which also shows the transmission spectrum of the bulk sample. The result reveals that there was almost no sign of meaningful transmission within the PBG for this line defect. This is consistent with our expectations based on the calculated dispersion curve.

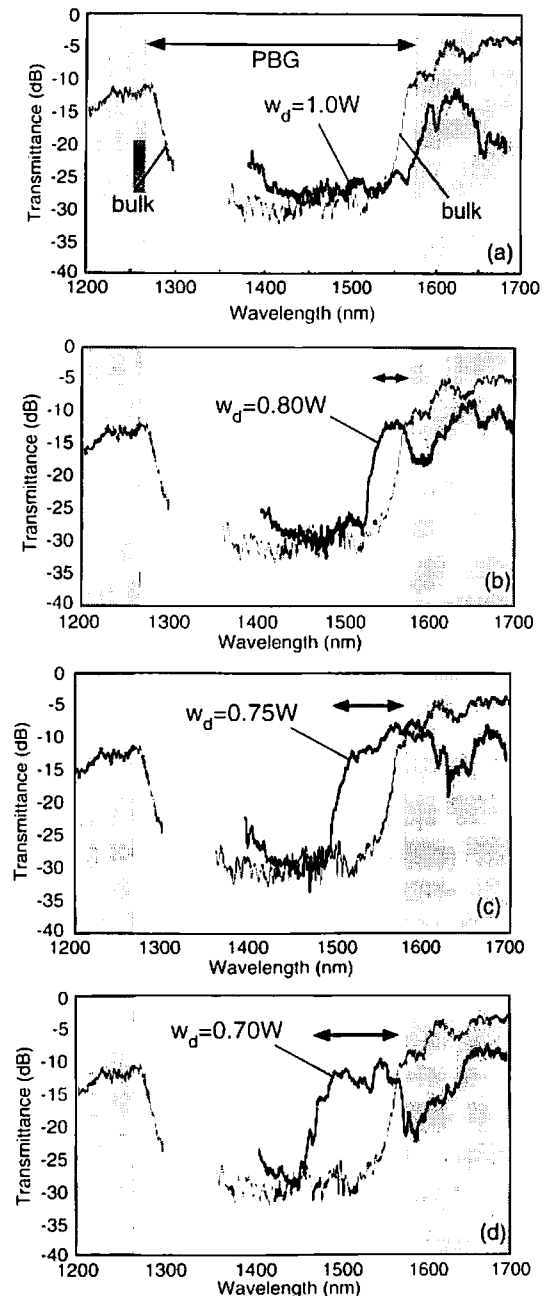


Fig. 5 Transmission spectra of line defects: (a) normal single-line defect ($w_d = 1.0W$), (b)–(d) width-reduced single-line defect ($w_d = 0.80, 0.75, 0.70W$). The dark shaded area corresponds to the region outside the PBG, and the pale shaded area corresponds to the transmission window where guided modes exist.

(b) Width-reduced line defects

Next, we examined width-reduced line defects. We prepared a series of line defects with w_d values varying from 0.65 to 0.85 W . Figures 5(b), (c), (d) show the transmission spectra of width-reduced line defects when $w_d = 0.80, 0.75$, and $0.70W$. The effect of the structural tuning is clearly seen in this spectrum. As w_d decreases, a transmission mode appears from the longer

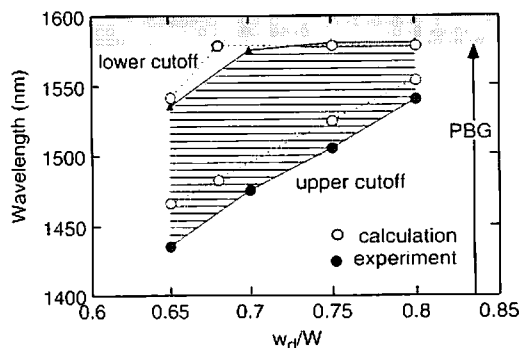


Fig. 6 Width dependence of transmission window. Experimental results and theoretical values are also shown.

wavelength edge of the PBG and shifts to the shorter wavelength region. The width of the transmission window is approximately 100 nm at $w_d = 0.7W$. When we compare the result in Fig. 5 with the theoretically calculated dispersion curves in Fig. 4, the observed w_d dependence can be understood in terms of a mode with a large group velocity entering the PBG region from the lower band edge.

To examine this in more in detail, we plot the transmission window as a function of w_d between 0.65 and 0.80 W in Fig. 6. The w_d dependence of an experimentally determined transmission window is fairly well explained by the theoretical calculation. This directly shows that the expected structural tuning is indeed realized in the fabricated line defect waveguides.

4. 3D Full Gap Photonic Crystal Fabrication

3D photonic crystals are much more difficult to fabricate than 2D photonic crystals. Furthermore, the requirement for the realization of a full gap in 3D is more severe than that in 2D. Thus, the reported methods for fabricating 3D photonic crystals with a full gap are fairly complicated [19], [20], and simpler fabrication methods are needed. We have recently proposed a new structure. This structure can be fabricated by a simple process that is a combination of alternating-layer deposition and two-step lithography [21].

Figure 7 shows the proposed structure and fabrication process, which is based on the autocloning bias-sputtering method [22] and the dry etching process. First, we fabricate 2D Si/SiO₂ periodic structures by alternating-layer bias-sputtering deposition in the autocloning mode. Then, we employ an additional lithography-and-etching process that provides vertical air through-holes into the 2D periodic structures. This structure is geometrically equivalent to a diamond lattice, which is known to possess a 3D full PBGT, and our band calculations using 3D plane-wave expansion revealed that our structure has a fairly large full PBG (approximately 12% of the center frequency).

The autocloning deposition method is powerful in

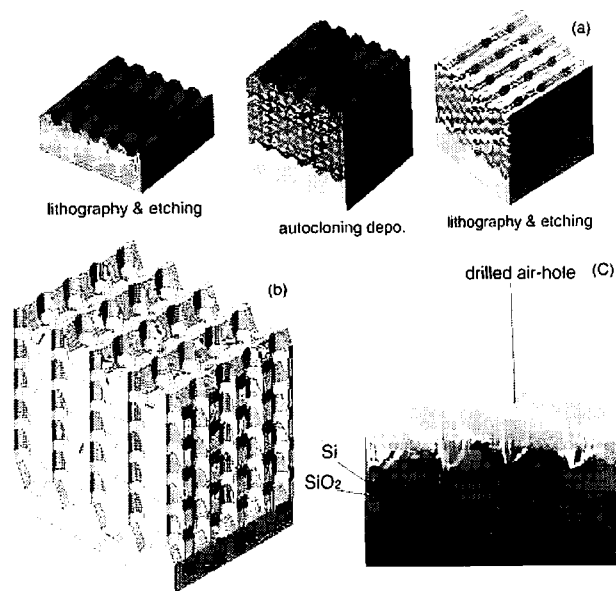


Fig. 7 Fabrication process (a) and schematic (b) of the proposed 3D drilled alternating-layer photonic crystal structure. SEM micrograph of a fabricated sample (c).

that it is capable of fabricating 2D or 3D periodic structures by a rather simple process (one-step deposition and one-step lithography). However, this alternating-layer deposition does not lead to full PBG because of the absence of connectivity in the vertical direction. The proposed fabrication method consists of a one-step deposition process and a two-step lithography process. This approach is much simpler than other methods developed to fabricate 3D full PBG materials.

Recently, we fabricated this type of photonic crystal that is designed for optical communication wavelengths by using e-beam lithography and ECR ion-stream dry etching [23]. Figure 7(b) shows the fabricated structure. This is still a preliminary result but this photograph shows that the proposed 3D geometrical structure can really be fabricated. Recently, we have characterized the optical transmittance of the crystal in the x , y , and z directions, and observed common dips in the transmittance spectra, suggesting the formation of gaps.

5. 3D/2D Hybrid Photonic Crystals

Full gap photonic crystals are ideal but it is not easy to incorporate functional defects in them and thus realize photonic crystal PICs. Therefore, we are also investigating 3D/2D hybrid photonic crystals as shown in Fig. 8, which can be fabricated by a process similar to that described in the previous section [24]. In this structure, PICs are formed in the 2D Si/air hexagonal air-hole photonic crystal layer sandwiched between 3D Si/SiO₂ photonic crystals. The photonic crystal itself

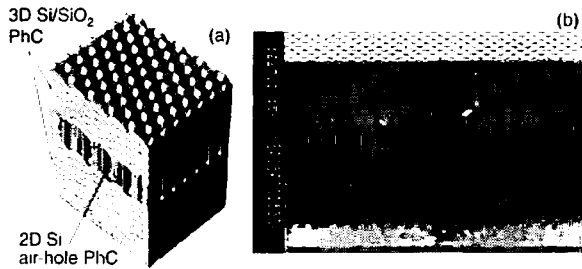


Fig. 8 Schematic of 3D/2D hybrid photonic crystals (a). SEM micrograph of the fabricated structure (b).

is the same as the Si photonic crystal slab described in Sect. 3, but here the cladding layers are 3D photonic crystals.

As mentioned above, a PIC structure may be 2D, and therefore we will need photonic crystals with a larger PBG within the 2D plane. Si/air photonic crystals have a large PBG within the 2D plane. 3D Si/SiO₂ photonic crystals do not have a large PBG in the 2D plane, but have a large PBG in the vertical direction. We expect this type of photonic crystal to be effective for controlling the radiation loss or emission process in a particular direction, which are difficult to accomplish with 2D slab structures.

A combination of the lithography-and-etching process and autocloning technology can enable us to fabricate this complicated structure. First, we fabricate 3D photonic crystals using the autocloning technology. Then, we fabricate periodic air holes on the top Si layer of the 3D photonic crystals using the lithography-and-etching process. Finally, we undertake additional autocloning deposition on this periodically patterned 2D surface, resulting in 3D Si/SiO₂ photonic crystals. An important point is that the upper 3D photonic crystals are identical to the lower ones because the autocloned surface shape does not depend on the depth of the initial corrugation. In addition, the air holes in the 2D photonic crystals are not buried during the final deposition by using a certain deposition mode.

We fabricated 3D/2D hybrid photonic crystals using the above method. Figure 8 shows an SEM micrograph of the fabricated structure. The fabricated structure is almost the same as the schematic figure.

This result shows that a combination of autocloning deposition and the lithography technique makes it possible to fabricate rather complicated photonic crystal structures. This technique may prove important in terms of realizing future photonic LSIs using photonic crystals.

6. Conclusion

In summary, we have shown three types of photonic crystals that are currently being investigated in our laboratories. As regards SOI photonic crystal slabs, we are

now able to fabricate various defect structures operating within the PBG frequency. The observed characteristics agree well quantitatively with theoretical calculations, and therefore the quantitative design of functional defect structures is now possible. The fabrication of 3D photonic crystals is still at a primitive stage, but a combination of lithography and deposition methods enables us to fabricate various types of 3D structures by a relatively simple process. The photonic crystal structures investigated in this paper have various merits and demerits and we believe that ultimately these three (or more) types of photonic crystal are needed to realize photonic-crystal-based PICs, and developed fabrication technologies will be used to realize future photonic LSIs.

We thank S. Ishihara, T. Tamamura, M. Morita, and H. Morita for their support.

References

- [1] J.D. Joannopoulos, R.D. Meade, and J.N. Winn, *Photonic Crystals*, Princeton University Press, 1995.
- [2] M. Notomi, "Theory of light propagation in strongly-modulated photonic crystals," *Phys. Rev. B*, vol.62, pp.10696-10705, 2000.
- [3] M. Kawachi, "Recent progress in silica-based planar light-wave circuits on silicon," *IEE Proc. Optoelectron.*, vol.143, pp.257-262, 1996.
- [4] O. Painter, R.K. Lee, A. Yariv, A. Scherer, J.D. O'Brien, P.D. Dapkus, and I. Kim, "Two-dimensional photonic bandgap defect mode laser," *Science*, vol.284, pp.1819-1824, 1999.
- [5] E. Chow, S.Y. Lin, S.G. Johnson, P.R. Villeneuve, J.D. Joannopoulos, J.R. Wendt, G.A. Vawter, W. Zubrzycki, H. Hou, and A. Alleman, "Three-dimensional control of light in a two-dimensional photonic crystal slab," *Nature*, vol.407, pp.983-986, 2000.
- [6] C. Takahashi, J. Takahashi, M. Notomi, and I. Yokohama, "Accurate dry etching with fluorinated gas for two-dimensional Si photonic crystals," 2000 Fall Meeting of Materials Research Society (MRS Proceedings, vol.637), E1.8, 2000.
- [7] C. Takahashi, Y. Jin, K. Nishimura, and S. Matsuo, "Anisotropic etching of Si and WSiN using ECR plasma of SF₆-CF₄ gas mixture," *Jpn. J. Appl. Phys.*, vol.39, pp.3672-3675, 2000.
- [8] A. Shinya, M. Notomi, I. Yokohama, C. Takahashi, and T. Tamamura, *Quantum Optoelectron.*, vol.34, pp.113-121, 2002.
- [9] N. Kawai, K. Inoue, N. Carlsson, N. Ikeda, Y. Sugimoto, K. Asakawa, and T. Takemori, "Confined band gap in an air-bridge type of two-dimensional AlGaAs photonic crystal," *Phys. Rev. Lett.*, vol.86, pp.2289-2292, 2001.
- [10] A. Shinya, M. Notomi, and I. Yokohama, "Finite thickness effect on slab-type asymmetrical two-dimensional photonic crystal waveguides," *OSA Topical Meeting of Integrated Photonic Research (IPR2000)*, p.186, Quebec, 2000.
- [11] I. Yokohama, M. Notomi, A. Shinya, C. Takahashi, and T. Tamamura, "Two-dimensional Si photonic crystals with 0.2 μm -thickness on oxide using SOI substrate," 5th Optoelectronics and Communications Conference (OECC2000), 11B2-4, 2000.
- [12] S. Noda, A. Chutinan, and M. Imada, "Trapping and emission of photons by a single defect in a photonic bandgap

- structure," *Nature*, vol.407, pp.608-611, 2000.
- [13] T. Baba, N. Fukaya, and J. Yonekura, "Observation of light propagation in photonic crystal optical waveguides with bends," *Electron. Lett.*, vol.35, pp.654-655, 1999.
 - [14] M. Loncar, D. Nedeljkovic, T. Doll, J. Vuckovic, A. Scherer, and T.P. Pearsall, "Waveguiding in planar photonic crystals," *Appl. Phys. Lett.*, vol.77, pp.1937-1939, 2000.
 - [15] A. Chutinan and S. Noda, "Waveguides and waveguide bends in a two-dimensional photonic crystal slab," *Phys. Rev. B*, vol.62, pp.4488-4492, 2000.
 - [16] A. Shinya, M. Notomi, K. Yamada, C. Takahashi, J. Takahashi, and I. Yokohama, "Two-dimensional Si-photonic crystal single mode waveguide on SiO₂ substrate which functions above the light line," *OSA Topical Meeting of Integrated Photonic Research (IPR 2001)*, IMD4, 2001.
 - [17] K. Yamada, H. Morita, A. Shinya, and M. Notomi, *Opt. Commun.*, vol.198, pp.395-402, 2001.
 - [18] M. Notomi, A. Shinya, K. Yamada, J. Takahashi, C. Takahashi, and I. Yokohama, "Singlemode transmission within photonic bandgap of width-varied single-line-defect photonic crystal waveguides on SOI substrate," *Electron. Lett.*, vol.37, pp.293-295, 2001.
 - [19] S. Noda, M.K. Tomoda, N. Yamamoto, and A. Chutinan, "Full three-dimensional photonic bandgap crystals at near-infrared wavelengths," *Science*, vol.289, pp.604-606, 2000.
 - [20] S.Y. Lin, J.G. Fleming, D.L. Hetherington, B.K. Smith, R. Biswas, K.M. Ho, M.M. Sigalas, W. Zubrzycki, S.R. Jurtz, and J. Bur, "A three-dimensional photonic crystal operating at infrared wavelengths," *Nature*, vol.394, pp.251-253, 1998.
 - [21] M. Notomi, T. Tamamura, T. Kawashima, and S. Kawakami, "Drilled alternating-layer three-dimensional photonic crystals having a full photonic band gap," *Appl. Phys. Lett.*, vol.77, no.26, pp.4256-4258, 2000.
 - [22] S. Kawakami, "Fabrication of submicrometre 3D periodic structures composed of Si/SiO₂," *Electron. Lett.*, vol.33, no.14, pp.1260-1261, 1997.
 - [23] E. Kuramochi, M. Notomi, T. Tamamura, T. Kawashima, S. Kawakami, C. Takahashi, and J. Takahashi, "Drilled alternating-layer structure for three-dimensional photonic crystals with a full band gap," *J. Vac. Sci. Technol. B*, vol.18, no.6, pp.3510-3513, 2000.
 - [24] E. Kuramochi, M. Notomi, T. Tamamura, C. Takahashi, J. Takahashi, T. Kawashima, and S. Kawakami, *Quantum Optoelectron.*, vol.34, pp.53-61, 2002.



Masaya Notomi was born in Kumamoto, Japan, on 16 February 1964. He received his B.E., M.E. and Dr.Eng. degrees in applied physics from University of Tokyo, Tokyo, Japan in 1986, 1988, and 1997, respectively. In 1988, he joined Nippon Telegraph and Telephone Corporation, NTT Optoelectronics Laboratories, Atsugi, Japan. Since then, his research interest has been to control the optical properties of materials and devices by using artificial nanostructures, and engaged in research on semiconductor quantum wires/dots and photonic crystal structures. He is currently a Distinguished Technical Member of NTT Basic Research Laboratories, Atsugi, Japan. From 1996-1997, he was with Linköping University, Sweden as a visiting researcher. Dr. Notomi is a member of the Japan Society of Applied Physics, and the American Physical Society.



Akihiko Shinya was born in Wakayama Prefecture, Japan, in 1971. He received the B.E., M.E. and Dr.Eng. degrees from Tokushima University, Japan, in 1994, 1996, and 1999, respectively. In 1999, he joined the NTT Basic Research Laboratories, Atsugi-shi, Japan. He has been engaged in research and development of Photonic crystal devices. Dr. Shinya is a member of the Japan Society of Applied Physics.



Eiichi Kuramochi was born in Ibaraki, Japan, in 1966. He received the B.E. and M.E. degrees in electrical engineering from Waseda University in 1989 and 1991, respectively. In 1991, he joined NTT Opto-electronics Laboratories, Atsugi-shi, Kanagawa, Japan, where he was engaged in research of semiconductor nano-structure for photonic devices. He is currently engaged in research of photonic crystals at NTT Basic Research Laboratories, Atsugi-shi, Kanagawa, Japan. He is a member of the Japan Society of Applied Physics.



Itaru Yokohama was born in Aomori, Japan, on January 13, 1959. He received the B.S., M.S., and Ph.D. degrees from Tokyo University, Tokyo, Japan, in 1981, 1983, and 1991, respectively. In 1983, he joined NTT Electrical Communication Laboratories, Ibaraki, Japan, where he engaged in research on fiber-optic components. Since 1987, he has been engaged in research on nonlinear optical devices and photonic crystals. He is now with NTT Basic Research Laboratories, Kanagawa, Japan. Dr. Yokohama is a member of the Japan Society of Applied Physics.



Chiharu Takahashi was born in Shizuoka Prefecture, Japan, on February 20, 1956. He received the B.S. and M.S. degrees from Nagoya University, Aichi, Japan, in 1979 and 1981, respectively. In 1981, he joined NTT Electrical Communication Laboratories, Tokyo, Japan. Since 1983, he engaged in research on ECR plasma and its application to fabrication processes of Si-LSI and GaAs IC. Since 1997, he has been engaged in research on

fabrication of optical microstructures photonic crystals. He is now with NTT Advanced Technology Corporation, Kanagawa, Japan. Mr. Takahashi is a member of the Japan Society of Applied Physics.



Koji Yamada was born in Fukuoka, Japan, in 1963. He received the M.S. degree in nuclear engineering from Kyushu University, Fukuoka, Japan, in 1988. Currently, he is a senior research engineer in NTT Telecommunications Energy Laboratories. In NTT's laboratories, he has engaged in theoretical and experimental studies on electron beam dynamics in storage rings for synchrotron radiation.

He has also engaged in studies on electromagnetic interaction between relativistic electrons and nano-scale multilayer structures. As well as these studies, he recently started studies on photonic crystal waveguides. His research interest is the application of relativistic electron beams to artificial nano-structures as photonic crystals.



Jun-ichi Takahashi was born in Osaka, Japan, in 1955. He took the Degree of M.E. in engineering science from Kyoto University, Japan, in 1982, and the Degree of Ph.D. in engineering from Tohoku University, Japan, in 1995. Currently, he is a senior research engineer in NTT Telecommunications Energy Laboratories. In NTT's laboratories, he has engaged in research for fabrication technology of silicon materials in non-thermal

equilibrium circumstances generated by synchrotron radiation or plasma excitation of reaction gases. He is also interested in abiotic synthesis of bio-organic compounds from primitive earth or planetary environment for exploring the origin and chemical evolution of life.



Takayuki Kawashima received B.E., M.E., and Ph.D. degrees in electronic engineering from Tohoku University, Sendai, Japan, in 1995, 1997, and 2000, respectively. From 1999 to 2001, he was a Research Fellow of the Japan Society for the Promotion of Science. Since 2001, he has been a Research Fellow of the New Industry Creation Hatchery Center (NICHe), Tohoku University. His current research interest is the development of the photonic

crystal devices and the process for fabricating photonic crystals. Dr. Kawashima is a member of the Japan Society of Applied Physics.



Shojiro Kawakami received the Ph.D. degree in 1965 from the University of Tokyo. He then joined Tohoku University. He was with Research Institute of Electrical Communication until 2000, and is with NICHe (New Industry Creation Hatchery Center). From late 60's to early 80's he worked mainly as a fiber optics theoretician. He switched the field to microoptics. Since late 1990's he is interested in photonic crystals. Prof.

Kawakami is a member of Japanese Optical Society and a Life Fellow, IEEE.